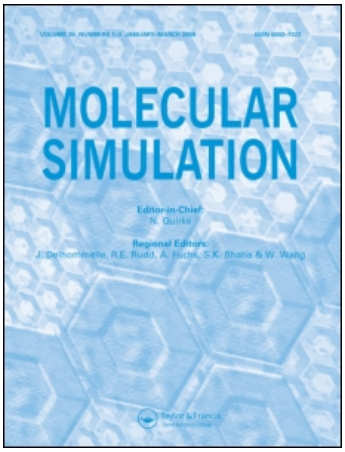


**Molecular Simulation**
Publication details, including instructions for authors and subscription information:
http://www.informaworld.com/smpp/title~content=t713644482

# Molecular-Dynamics Simulations for the Density Autocorrelation Function in a Supercooled Fluid Phase

K. Uehara[a]; T. Muranaka[a]; H. Miyagawa[ab]; M. Takasu[a]; Y. Hiwatari[a]
[a] Department of Physics, Faculty of Science, Kanazawa University, Kanazawa, Ishikawa, Japan [b] Integral Research Institute, Taisho Seiyaku Co., Ltd, Ohmiya, Saitama, Japan

**To cite this Article** Uehara, K. , Muranaka, T. , Miyagawa, H. , Takasu, M. and Hiwatari, Y.(1994) 'Molecular-Dynamics Simulations for the Density Autocorrelation Function in a Supercooled Fluid Phase', Molecular Simulation, 12: 3, 253 — 270
**To link to this Article: DOI:** 10.1080/08927029408023035
**URL:** http://dx.doi.org/10.1080/08927029408023035

*Molecular Simulation*, 1994, Vol. 12(3-6), pp. 253-270
Reprints available directly from the publisher
Photocopying permitted by license only



# MOLECULAR-DYNAMICS SIMULATIONS FOR THE DENSITY AUTOCORRELATION FUNCTION IN A SUPERCOOLED FLUID PHASE

K. UEHARA, T. MURANAKA, H. MIYAGAWA†, M. TAKASU and Y. HIWATARI

*Department of Physics, Faculty of Science, Kanazawa University, Kanazawa, Ishikawa 920-11, Japan*
*†Integral Research Institute, Taisho Seiyaku Co., Ltd, Ohmiya, Saitama 330, Japan*

*(Received March 1993, accepted May 1993)*

We have re-calculated the self part of the density autocorrelation function $F_s(k, t)$ (incoherent scattering function) for the binary soft-sphere fluid with a much longer molecular-dynamics (MD) simulation than our previous MD calculations, and with a larger system size ($N = 4000$) to a longer time window as well as to study a system-size dependence, if it exists. The full density autocorrelation function $F(k, t)$ was also computed. It is found that all $F(k, t)$'s that we have computed in this work can be fitted over a wide range of time steps (at least over three figures of the decay) by a Williams-Watts stretched exponential function $F_s(k, t) = A \exp[-(t/t_0)^{\beta}]$, where $A$, $\beta$ and $t_0$ are adjustable parameters. Other significant dynamical behaviours were also presented in mean square displacements and non-Gaussian parameters for highly supercooled fluids with $N = 4000$. The present results are compatible to our previous computations with $N = 500$, but a significant size dependence is suggested.

KEY WORDS: Density autocorrelation function, $\alpha$ relaxation, stretched exponential decay



## 1 INTRODUCTION

When a fluid is cooled down below the freezing temperature rapidly enough to prevent a nucleation which will lead to crystallization of the fluid, the system stays in a supercooled fluid state; the supercooled fluid exhibits a typical slow relaxation phenomenon [1], which is possibly observed by incoherent and coherent neutron scattering (density fluctuations) experiments on the dynamic structure factor $S(k, \omega)$. In this paper, we have re-calculated the self part of the density autocorrelation function $F_s(k, t)$ (incoherent scattering function), which is the Fourier transform of $S_s(k, \omega)$ with respect to $\omega$, for a binary soft-sphere fluid with a much longer molecular-dynamics (MD) simulation than our previous MD calculations [2-5], and with a larger system size to obtain more accurate informations on slow relaxations of the function as well as to study a system-size dependence, if it exists. The full density autocorrelation function $F(k, t)$ is also computed. It is found that all $F_s(k, t)$'s that we have computed in this work can be fitted over a wide range of time steps (at least over three figures of decay) by the Williams-Watts stretched exponential function $F_s(k, t) = A \exp[-(t/t_0)^{\beta}]$ except for a very short time region, where $A$, $\beta$ and $t_0$ are adjustable parameters.

When $\beta$ is less than unity, the system is accompanied by slow relaxations in the sense that the time ratio for the relaxation function to become $1/e$ times an initial value strongly increases as the time increases. It has been obtained by the MD simulations for the binary soft-sphere model, which we consider again in the present work, that the value of $\beta$ begins to deviate from unity, as the coupling constant $\Gamma_{\text{eff}}$ (see Equation (2)) increases, around when $\Gamma_{\text{eff}} \simeq 1.45 \simeq \Gamma_c$, where $\Gamma_c$ is a kinetic transition predicted by the trapping diffusion model [1, 5–10]. We also look into system-size dependence of the results of the molecular-dynamics simulation.

In our previous works [2–4] we have already computed $F_s(k, t)$ for various $k$'s and $\Gamma_{\text{eff}}$'s in the time window of the order of $100\tau$, where $\tau$ is a microscopic time scale determined by the potential parameters and the mass of particles (see next section for the definition) and with $N$ (system size) = 500. However, since the system exhibits significant slowing-down phenomena in a temperature region in which we are interested, such time window is too short for the relaxation function to fully be damped. Therefore, we have carried out the present MD simulation in order to extend our previous molecular-dynamics computations to, at least, one order of magnitude longer time steps, which will definitely be useful to our better understandings of the slow dynamics in both moderately and highly supercooled states.



## II BINARY SOFT-SPHERE MODEL AND THE MOLECULAR-DYNAMICS SIMULATIONS

As a simple model for binary alloys, we consider in our MD simulation soft-sphere mixtures composed of $N_1$ atoms of mass $m_1$ and diameter $\sigma_1$ and $N_2$ atoms of mass $m_2$ and diameter $\sigma_2$ in a volume $V$, which interact through the purely repulsive soft-sphere potentials [11–13]:

$$v_{\alpha\beta}(r) = \varepsilon\left(\frac{\sigma_{\alpha\beta}}{r}\right)^{12}, \tag{1}$$

where $1 \leq \alpha, \beta \leq 2$ are species indices, $\epsilon$ is the energy unit, and we simply assume that $\sigma_{\alpha\beta} = (\sigma_\alpha + \sigma_\beta)/2$.

According to the scaling property of the inverse power potentials, it is easily shown that all reduced equilibrium properties of the soft-sphere mixtures, in excess of their ideal gas counterpart, depend only on the coupling constant $n^*(T^*)^{-1/4}$ apart from the core size ratio $\sigma_2/\sigma_1$ and the concentration $x_1$ or $x_2$, where $n^* = N\sigma_1^3/V$ denotes the reduced number density with the total number of atoms $N(=N_1 + N_2)$. The reduced temperature $T^*$ equals $k_B T/\varepsilon$, $x_1 = N_1/N$ and $x_2 = 1 - x_1$. However, it is useful to use the following effective coupling constant for binary mixtures, using an effective one-component approximation:

$$\Gamma_{\text{eff}} = n^*(T^*)^{-1/4}\left(\frac{\sigma_{\text{eff}}}{\sigma_1}\right)^3, \tag{2}$$

$$\sigma_{\text{eff}}^3 = \sum_\alpha \sum_\beta x_\alpha x_\beta \sigma_{\alpha\beta}^3. \tag{3}$$

The equation of states (compressibility factor $PV/Nk_BT$ vs $\Gamma_{eff}$) for binary soft-spheres has been found to follow the curve very close to that of the pure soft-sphere model [11, 12], which implies that the effective one-component approximation works very well. The freezing point of the pure soft-sphere model has been found to occur at $\Gamma_{eff} = 1.15$.

In the present work, we study a binary soft-sphere mixture with the core-size ratio $\sigma_2/\sigma_1 = 1.2$, mass ratio $m_2/m_1 = 2.0$, and an equimolar system ($x_1 = 0.5$). Using the constant-temperature MD techniques and the seventh-order Gear algorithm together with periodic boundary conditions as usual, we have carried out MD simulations with $N = 4000$ particles in a cubic cell as well as with $N = 500$ to see a system-size dependence, if it exists. The pair potential, Equation (1), is cut off over the distance $r/\sigma_{\alpha\beta} = 3.5$, and the number density was kept constant ($n^* = 0.8$); the temperature $T^*$ was varied to achieve desired $\Gamma_{eff}$'s. The microscopic time scale is chosen to be

$$\tau = \left(\frac{m_1\sigma_1^2}{\varepsilon}\right)^{1/2}, \tag{4}$$

which is nearly the same order of magnitude of the Einstein period of oscillation of atoms in an equivalent solid. This becomes of the order of $10^{-13}$ sec, if we used the parameters for an argon liquid in Equation (4). The equation of motions were solved numerically with a time mesh of the order of 100th of $\tau$, which precisely depends on the respective temperature.

First, we simulated an equilibrium fluid of $\Gamma_{eff} = 0.8$; then, using the configuration at the final step of this run, this fluid was quenched down to $\Gamma_{eff} = 1.6$ (quenching process). The resulting cooling rate is equivalent to of the order of $10^{13}$ K/sec for an argon fluid, which is much faster than those achieved by experimental techniques.

Annealing MD simulation has been carried out for various different $\Gamma_{eff}$'s, starting with the final configuration of the corresponding $\Gamma_{eff}$ obtained by the quenching MD simulation mentioned above.



## III DENSITY AUTOCORRELATION FUNCTION

Density autocorrelation function (DAF) $F^{(\alpha)}(k, t)$ of species $\alpha$, defined below, measures how intrinsically excited density fluctuations associated with a wavenumber $k$ relaxes with an elapsed time $t$.

$$F^{(\alpha)}(k, t) = \frac{1}{N_\alpha}\langle \rho^{(\alpha)}(\mathbf{k}, t)\rho^{(\alpha)}(-\mathbf{k}, 0)\rangle, \tag{5}$$

where

$$\rho^{(\alpha)}(\mathbf{k}, t) = \sum_{i=1}^{N_\alpha} \exp\left(i\mathbf{k}\cdot\mathbf{r}_i^{(\alpha)}(t)\right) \tag{6}$$

are the density fluctuations associated with wavenumber $k$. $F^{(\alpha)}(k, t)$ is sometimes called a total density autocorrelation. On the other hand, the self part of it, $F_s^{(\alpha)}(k, t)$, can be written as:

$$F_s^{(\alpha)}(k,t) = \frac{1}{N_\alpha}\sum_{i=1}^{N_\alpha}\langle \exp\{i\mathbf{k}\cdot[\mathbf{r}_i^{(\alpha)}(t) - \mathbf{r}_i^{(\alpha)}(0)]\}\rangle. \tag{7}$$

We have calculated both $F^{(\alpha)}(k,t)$ and $F_s^{(\alpha)}(k,t)$ for various $\Gamma_{\text{eff}}$'s and $k$'s. Since the side length of the cubic simulation cell is finite, $k$ can not be smaller than $k_1 = 2\pi/L$ with $L = V^{1/3}$.

We have attempted to fit the MD data of $F_s^{(\alpha)}(k,t)$ in terms of the stretched exponential function of the form of the Williams-Watts law:

$$f(t) = A\exp[-(t/t_0)^\beta]. \tag{8}$$

The result of the best fitting for $k = k_1$ indicates that $\beta \simeq 1$ up to $\Gamma_{\text{eff}} = 1.40$ and that the hydrodynamic relation $t_0 = (Dk^2)^{-1}$ is nearly satisfied within an accuracy of the data for this range of $\Gamma_{\text{eff}}$, where $D$ is the self-diffusion coefficient [1,3,4,13]. Thus, the MD simulation confirms the normal relaxation (simple exponential decay and hydrodynamic relation) for the supercooled fluids of binary soft spheres up to $\Gamma_{\text{eff}} \leq 1.40$. A significant change is obtained around $\Gamma_{\text{eff}} = 1.45$, above which $\beta$ becomes significantly smaller than one and the hydro-dynamic

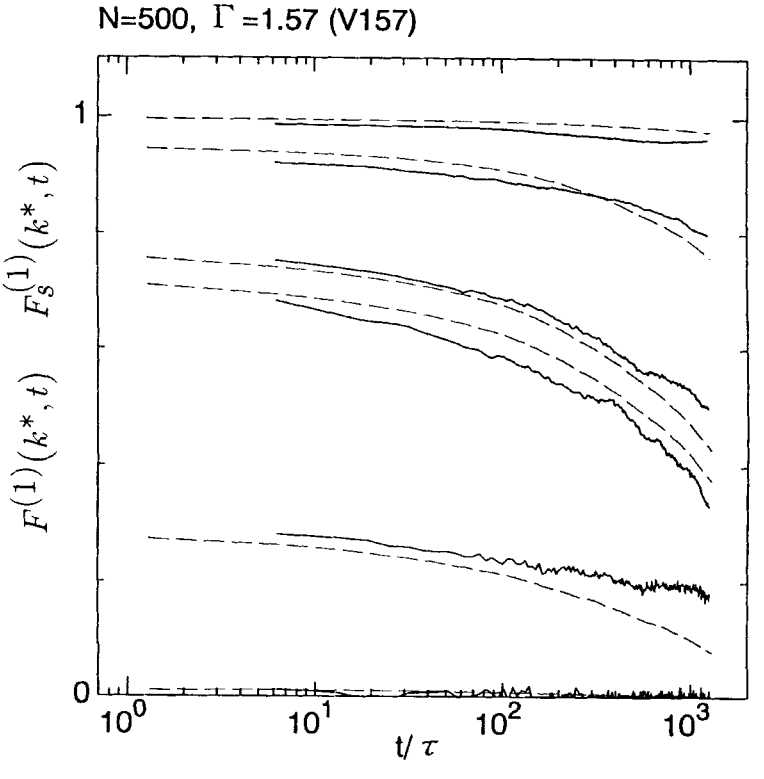


**Figure 1** The full and self-part density autocorrelation functions (the lighter species only), $F^{(1)}(k^*, t)$ (wavy curves) and $F_s^{(1)}(k^*, t)$ (dashed curves), for the binary soft-sphere fluid at $\Gamma_{\text{eff}} = 1.57$, close to the liquid-glass transition point $\Gamma_g(=1.58)$, obtained by the molecular dynamics simulation with $N = 500$. $k^* = 1$, 4, 9, 10, 20, and 40 from the top, where $k^*$ is the reduced wavenumber defined as $k^* = k[\frac{2\pi}{L}]^{-1}$. The functions are not shown for $t/\tau < 1$.

relation no more holds. This indicates a remarkable slowing down of kinetics already takes place around $\Gamma_{\text{eff}} \simeq 1.45$, which is substantially smaller than the liquid-glass transition $\Gamma_g (=1.58)$ [1, 6]. This is consistent with the behavior of the mean-squared displacement (MSD) which will be mentioned below. Such drastic changes of kinetics around $\Gamma_{\text{eff}} \simeq 1.45$ may be regarded as a kinetic transition [8], but we should note that this can not be identified as the glass transition of the system, because the diffusivity (viscosity) is still too large (small), compared with a typical value of a solid.

Figure 1 shows both $F^{(1)}(k, t)$ and $F_s^{(1)}(k, t)$ vs. log $t/\tau$ at $\Gamma_{\text{eff}} = 1.57$ for different $k$'s. Note that both functions at each $k$ behaves quite similarly, though the former function is less accurate than the latter. The decay of the functions at large times, which is called $\alpha$ relaxation, looks not significantly different for $F^{(1)}(k, t)$ and $F_s^{(1)}(k, t)$. Thus, we see that the $\alpha$ relaxation is essentially the same for both $F^{(\alpha)}(k, t)$ and $F_s^{(\alpha)}(k, t)$, and therefore, we will study below in detail only the self part, which is more easily as well as more accurately obtained than the total density autocorrelation function. Figure 2 shows the self part of the density autocorrelation function $F_s^{(1)}(k, t)$ at $\Gamma_{\text{eff}} = 1.57$ for various $k$'s, obtained by our MD simulations

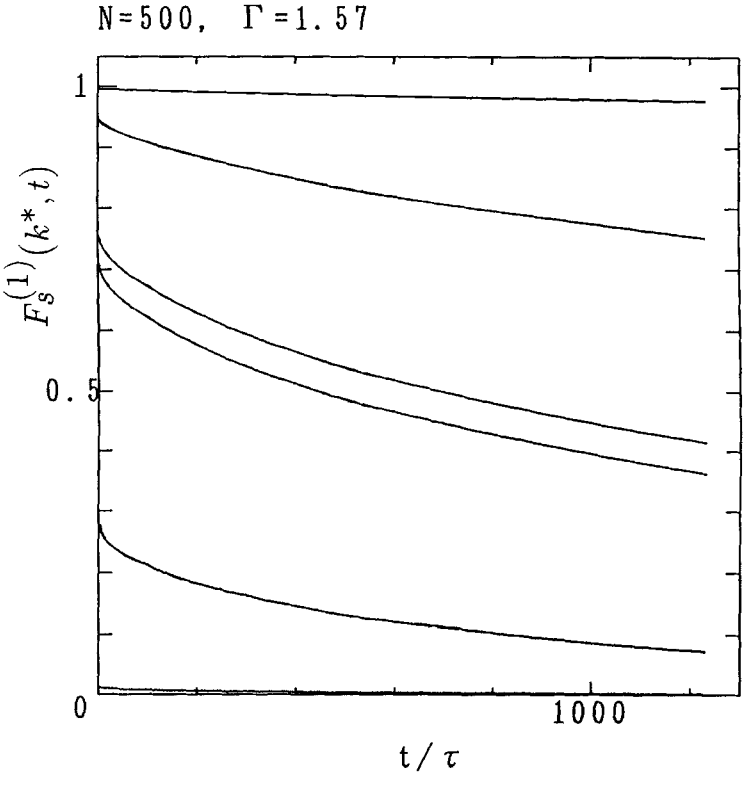


**Figure 2** $F_s^{(1)}(k^*, t)$ at $\Gamma_{\text{eff}} = 1.57$. $N = 500$ and $k^* = 1$, 4, 9, 10, 20 and 40 from the top. The solid curves are the MD results, while the dashed curves, almost overlapped into each solid curves, are the results obtained by the least square fittings with the form of the stretched exponential function, Equation (8).

with $N = 500$. The MD data are best fitted in terms of the stretched exponential function, Equation (8). The result of the fitting turns out to be perfect, since both the MD data and the fitting curves are nearly on the same curve for each $k$ over the whole range of the time window shown there except for very short times. Results on the values of the parameters in the stretched exponential function by these fittings are summarized in Table 1, and the value of the exponent $\beta$ as a function of $\Gamma_{\text{eff}}$ is also shown in Figure 3, for which $k(=\frac{2\pi}{L})$ is the minimum wavenumber compatible with the side length $(L)$ of a cubic simulation cell $(L^3)$. It is obtained that $\beta = 1$ for $\Gamma_{\text{eff}} \leq 1.4$, while $\beta < 1$ for $\Gamma_{\text{eff}} \geq 1.45$.

Now, we study a larger system size; MD results on $F_s^{(\alpha)}(k, t)$ for $\Gamma_{\text{eff}} = 1.45$, 1.50, 1.55, and 1.60 obtained with $N = 4000$ are shown in Figures 4–7 and in Table 2. Again, we see that the MD data are well fitted by the stretched exponential function for all cases that was studied in this work. Comparison between Tables 1 and 2 could give us a system-size dependence of the MD results. Here, we note that $k = 2\pi k^*/L$ is proportional to the inverse of the side length of the cubic simulation cell $L$. Therefore, when the value of $k^*$ is the same either $N = 500$ or $N = 4000$, a corresponding $k$ value is half smaller for $N = 4000$ than that for $N = 500$. The

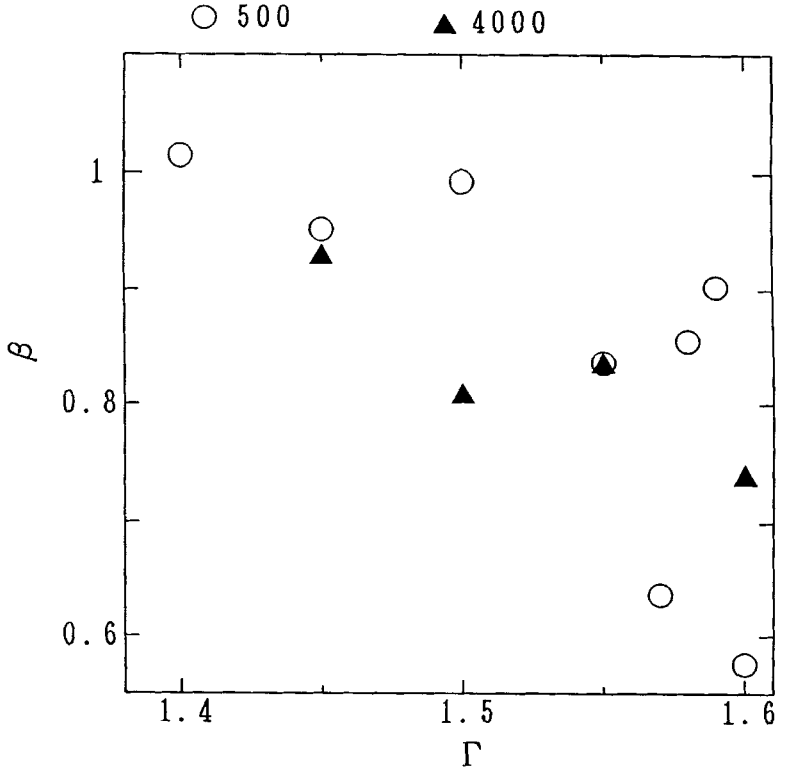


**Figure 3** $\beta$ vs $\Gamma_{\text{eff}}$. Circles are the results with $N = 500$, while triangles are with $N = 4000$; the values of $\beta$ are calculated by the least-square fittings with Equation (8), where $k^* = 1$ for $N = 500$ and $k^* = 4$ for $N = 4000$.

**Table 1** Results of the least-square fittings for $F_s^{(\alpha)}(k, t)$ at various $k^*$s obtained from the MD simulations with $N = 500$, using the stretched exponential function of the form, Equation (8). Values of $t_0$ are in the units of $\tau$. Last column means the sum of squared error (difference in values between the MD data and the best-fitted stretched exponential function at each point (every 400 time steps)).

$k^* = 1.0$

| $\Gamma$ | $A$ | $t_0$ | $\beta$ | $error^2$ |
|---|---|---|---|---|
| 1.40 | 0.99219 | 1114.66 | 1.01453 | 7.77E-05 |
| 1.45 | 0.99544 | 3981.28 | 0.95243 | 3.23E-04 |
| 1.50 | 0.99443 | 11400.86 | 0.99286 | 1.02E-04 |
| 1.55 | 0.99609 | 86423.41 | 0.83545 | 3.66E-06 |
| 1.57 | 0.99743 | 553292.28 | 0.63604 | 3.59E-05 |
| 1.58 | 0.99633 | 470813.24 | 0.85449 | 1.66E-06 |
| 1.59 | 0.99650 | 78811.55 | 0.90263 | 5.27E-06 |
| 1.60 | 0.99701 | 5674699.80 | 0.57548 | 1.04E-05 |

$k^* = 4.0$

| $\Gamma$ | $A$ | $t_0$ | $\beta$ | $error^2$ |
|---|---|---|---|---|
| 1.40 | | | | |
| 1.45 | | | | |
| 1.50 | 0.92824 | 1138.44 | 0.85513 | 1.17E-02 |
| 1.55 | 0.99610 | 4624.54 | 0.81006 | 1.07E-03 |
| 1.57 | 0.95064 | 11438.82 | 0.64899 | 1.33E-03 |
| 1.58 | 0.94507 | 46022.67 | 0.72777 | 2.05E-04 |
| 1.59 | 0.94424 | 5569.32 | 0.86548 | 4.28E-04 |
| 1.60 | 0.95495 | 136886.34 | 0.49519 | 2.30E-03 |

$k^* = 9.0$

| $\Gamma$ | $A$ | $t_0$ | $\beta$ | $error^2$ |
|---|---|---|---|---|
| 1.40 | | | | |
| 1.45 | | | | |
| 1.50 | 0.69048 | 486.57 | 0.70903 | 8.08E-03 |
| 1.55 | 0.73316 | 1642.31 | 0.70093 | 7.23E-03 |
| 1.57 | 0.75527 | 2745.77 | 0.64312 | 1.08E-03 |
| 1.58 | 0.76717 | 48301.91 | 0.49295 | 1.06E-03 |
| 1.59 | 0.75292 | 2043.50 | 0.79766 | 2.64E-03 |
| 1.60 | 0.80179 | 37889.22 | 0.36560 | 2.09E-02 |

$k^* = 10.0$

| $\Gamma$ | $A$ | $t_0$ | $\beta$ | $error^2$ |
|---|---|---|---|---|
| 1.40 | | | | |
| 1.45 | | | | |
| 1.50 | 0.63832 | 428.14 | 0.69035 | 7.98E-03 |
| 1.55 | 0.68220 | 1433.48 | 0.69998 | 9.65E-03 |
| 1.57 | 0.70673 | 2324.87 | 0.64550 | 1.24E-03 |
| 1.58 | 0.72347 | 46624.50 | 0.47078 | 1.17E-03 |
| 1.59 | 0.70772 | 1825.49 | 0.78294 | 3.14E-03 |
| 1.60 | 0.76072 | 29830.86 | 0.35627 | 2.33E-02 |

**Table 1** cont.

$k^* = 20.0$

| $\Gamma$ | $A$ | $t_0$ | $\beta$ | $error^2$ |
|---|---|---|---|---|
| 1.40 | | | | |
| 1.45 | | | | |
| 1.50 | 0.20835 | 155.34 | 0.61567 | 1.17E-03 |
| 1.55 | 0.25282 | 544.33 | 0.66352 | 3.22E-03 |
| 1.57 | 0.27040 | 832.90 | 0.65833 | 1.78E-03 |
| 1.58 | 0.30021 | 12402.20 | 0.43835 | 1.53E-03 |
| 1.59 | 0.28436 | 815.30 | 0.74037 | 1.60E-03 |
| 1.60 | 0.33459 | 4436.93 | 0.33423 | 1.01E-02 |

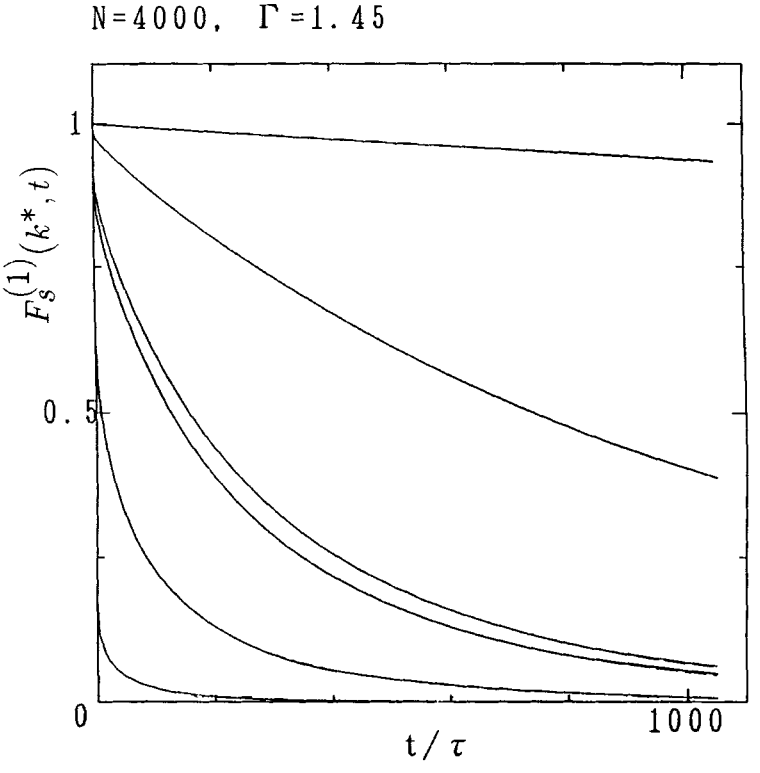


**Figure 4** $F_s^{(1)}(k^*, t)$ at $\Gamma_{\text{eff}} = 1.45$. The solid curves are the results of the MD simulations with $N = 4000$ for $k^* = 1$, 4, 9, 10, 20, and 40. Note that these values are the same as those of Figure 2, but the corresponding wavenumber $k$ is the half of each previous value because of the system-size difference.

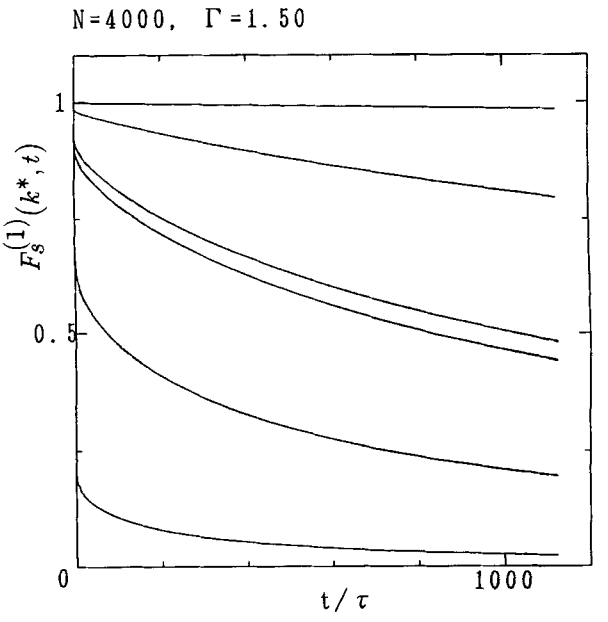


**Figure 5** The same as Figure 4, but for $\Gamma_{eff} = 1.50$.

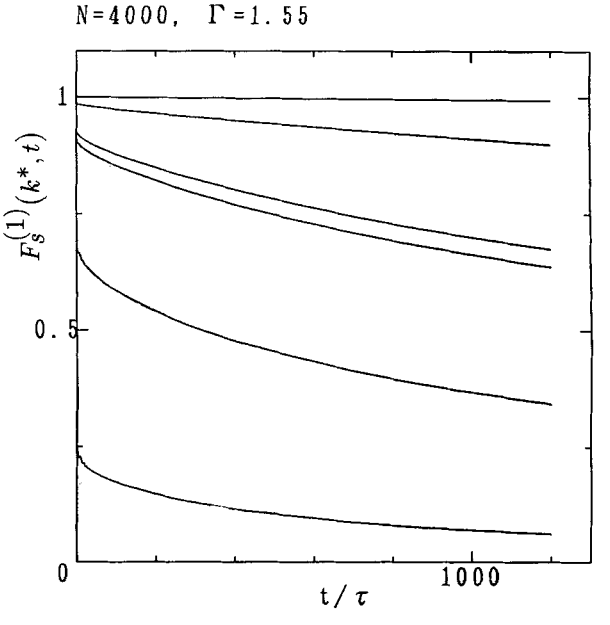


**Figure 6** The same as Figure 4, but for $\Gamma_{eff} = 1.55$.

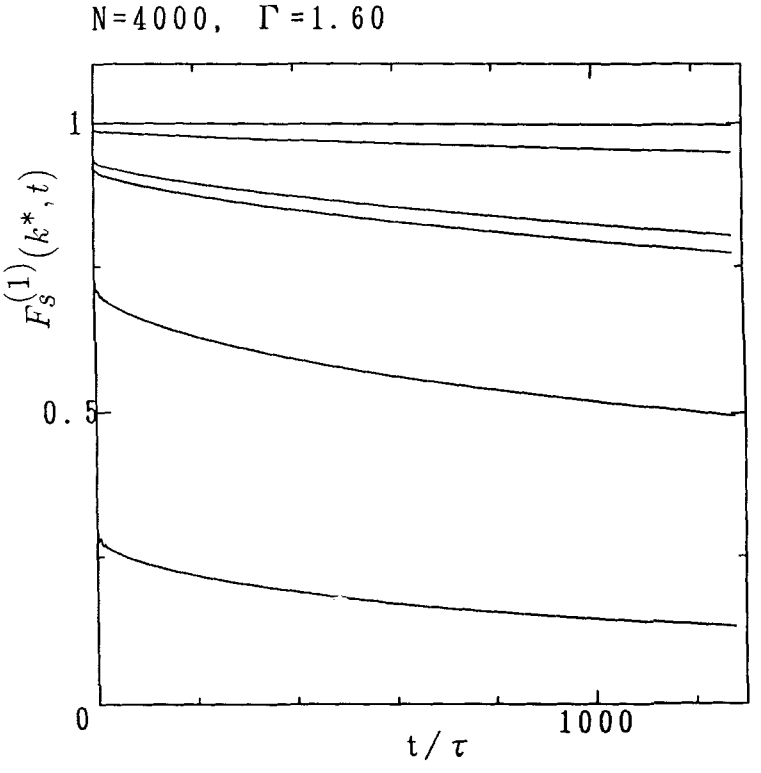


**Figure 7** The same as Figure 4, but for $\Gamma_{eff} = 1.60$.



system-size dependence of the best-fit results on the value of $\beta$ is also shown in Figure 3. It is noticeable that the results with $N = 4000$ look more systematic in its $\Gamma_{eff}$ dependence than those with $N = 500$, which are rather scattered in it. All these results obtained clearly indicate that the value of $\beta$ strongly depends on the thermodynamic variable $\Gamma_{eff}$. Thus, $F_s^{(\alpha)}(k, t)$ does not scale simply $t/t_0$. This result is not consistent with the simple scaling relation based on the neutron scattering experiment [14]. However, recent report [15] suggest a temperature dependence of $\beta$ similar to the present MD results.

## IV MEAN SQUARE DISPLACEMENTS AND NON-CAUSSIAN PARAMETERS

The self part of the density autocorrelation function, $F_s^{(\alpha)}(k, t)$, can generally be expanded into powers of $k^2$ (cumulant expansion) [16]:

$$F_s^{(\alpha)}(k, t) = \exp\left[ -\frac{1}{6}k^2 R_\alpha(t) + \frac{1}{72}k^4 [R_\alpha(t)]^2 A_\alpha(t) + \mathcal{O}(k^6) \right], \qquad (9)$$

**Table 2** Results of the least-square fittings for $F_s^{(1)}(k, t)$ at various $k^*$'s obtained from the MD simulations with $N = 4000$, using the stretched exponential function of the form, Equation (8). Values of $t_0$ are in the units of $\tau$. Last column means the sum of squared error (difference in values between the MD data and the best-fitted stretched exponential function at each point (every 400 time steps)).

$k^* = 1.0$

| $\Gamma$ | $A$ | $t_0$ | $\beta$ | $error^2$ |
|---|---|---|---|---|
| 1.45 | 0.99862 | 18072.03 | 0.95313 | 1.18E-06 |
| 1.50 | 0.99885 | 150732.35 | 0.85301 | 1.91E-07 |
| 1.55 | 0.99892 | 419438.00 | 0.86532 | 8.42E-08 |
| 1.60 | 0.99913 | 3314359.38 | 0.75274 | 4.28E-08 |

$k^* = 4.0$

| $\Gamma$ | $A$ | $t_0$ | $\beta$ | $error^2$ |
|---|---|---|---|---|
| 1.45 | 0.97782 | 1140.70 | 0.92818 | 1.97E-04 |
| 1.50 | 0.98265 | 7721.81 | 0.80623 | 8.54E-05 |
| 1.55 | 0.98321 | 21519.50 | 0.83282 | 1.19E-05 |
| 1.60 | 0.98617 | 102047.85 | 0.73766 | 6.80E-06 |

$k^* = 9.0$

| $\Gamma$ | $A$ | $t_0$ | $\beta$ | $error^2$ |
|---|---|---|---|---|
| 1.45 | 0.90399 | 299.78 | 0.80293 | 2.05E-03 |
| 1.50 | 0.92015 | 2109.72 | 0.68097 | 1.68E-03 |
| 1.55 | 0.92155 | 5822.43 | 0.73399 | 2.65E-04 |
| 1.60 | 0.93237 | 20698.06 | 0.68417 | 6.68E-05 |

$k^* = 10.0$

| $\Gamma$ | $A$ | $t_0$ | $\beta$ | $error^2$ |
|---|---|---|---|---|
| 1.45 | 0.88500 | 257.63 | 0.77518 | 2.58E-03 |
| 1.50 | 0.90212 | 1848.92 | 0.66030 | 1.78E-03 |
| 1.55 | 0.90478 | 5117.14 | 0.71418 | 3.86E-04 |
| 1.60 | 0.91749 | 17757.57 | 0.67029 | 8.51E-05 |

$k^* = 20.0$

| $\Gamma$ | $A$ | $t_0$ | $\beta$ | $error^2$ |
|---|---|---|---|---|
| 1.45 | 0.62236 | 95.64 | 0.61985 | 2.16E-03 |
| 1.50 | 0.66398 | 762.10 | 0.53188 | 1.97E-03 |
| 1.55 | 0.68282 | 2225.38 | 0.59543 | 1.50E-03 |
| 1.60 | 0.71974 | 7436.90 | 0.55695 | 5.33E-04 |

where $R_\alpha(t)$ and $A_\alpha(t)$ are the mean square displacement and non-Gaussian parameter for $\alpha$ species, respectively, which are defined as [1, 4, 13]

$$R_\alpha(t) = \langle |\mathbf{r}_i^{(\alpha)}(t) - \mathbf{r}_i^{(\alpha)}(0)|^2 \rangle, \tag{10}$$

(11)

$$A_\alpha(t) = \frac{3}{5} \frac{\langle |\mathbf{r}_i^{(\alpha)}(t) - \mathbf{r}_i^{(\alpha)}(0)|^4 \rangle}{[R_\alpha(t)]^2} - 1. \tag{12}$$

Here, $\langle \cdots \rangle$ stands for the average over configurations $\{\mathbf{r}_i\}$.

The mean square displacements for each species, $\alpha = 1, 2$, for $\Gamma_{\text{eff}} = 1.45 \sim 1.60$ are shown in Figures 8 through 11. As can easily be seen from these figures, $R_\alpha$ are never reached to a t-linear behaviour in the time scales shown there; they are still bent downwards over the time scales $10^3 t/\tau$. This is a remarkable contrast to lower $\Gamma_{\text{eff}}$'s, for which $R_\alpha(t)$ easily reaches a t-linear behaviour in much shorter time scales than the present [1, 4]. The dynamical nature seen in these figures is

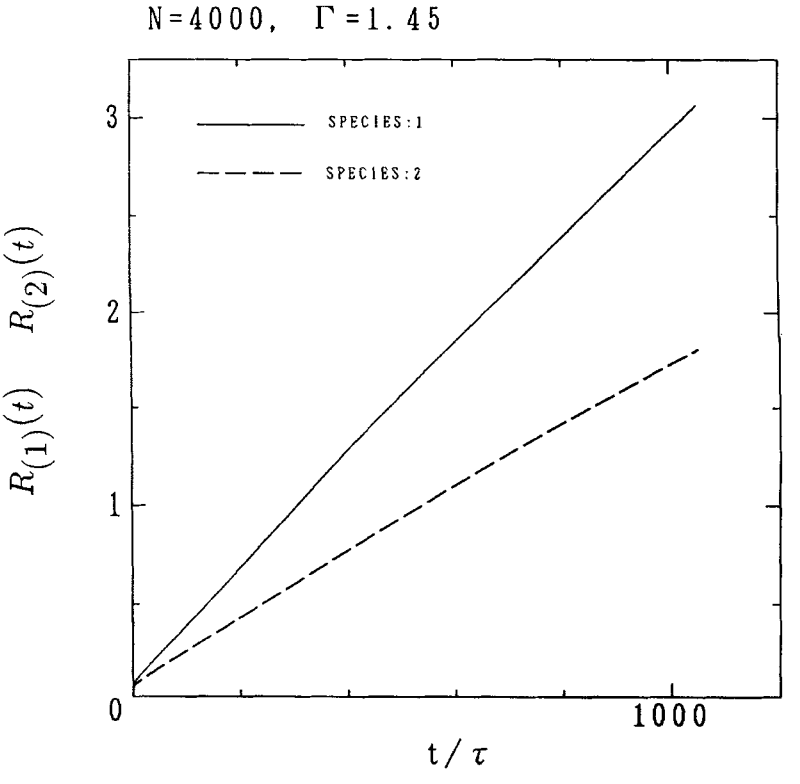


**Figure 8** Mean square displacements (MSD) in units of $\sigma_1^2$ for the binary soft-sphere model; the solid curve for the lighter species and the dashed curve for the heavier species. Note that the MSD intersects at the origin, since $R_\alpha = 0$ at $t = 0$ by the definition. It is only for appearance that the curves do not start with the origin in the time scales shown here.

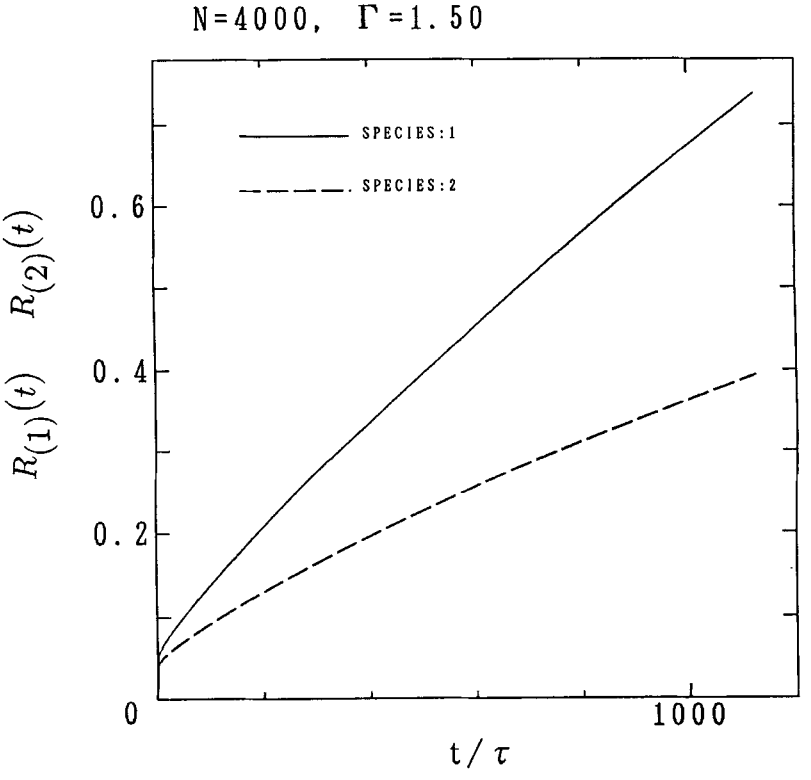


**Figure 9** The same as Figure 8, but for $\Gamma_{eff} = 1.50$.



essentially equivalent to the slow dynamics already observed in $F_s^{(\alpha)}(k, t)$, when $k$ is sufficiently small. This is easily understood by Equation (9), which is more clearly stated as follows: Since $A_\alpha$ is of the order of one, the ratio of the second term to the first term is approximately of the order of $k^2R_\alpha(t)$. Therefore, the second term of the cumulant expansion in $F_s^{(\alpha)}(t)$ can be neglected when $k^2R_\alpha(t) \ll 1$. This condition is satisfied when $k\sigma_1 < 1$ for the our cases, in which $R_\alpha \sim 1$ or $R_\alpha(t) < 1$ (see Figures 8–11).

Figures 12 to 15 show the non-Gaussian parameter obtained from the present MD simulation with $N = 4000$ for $\Gamma_{eff} = 1.45$, 1.50 1,55, and 1.60. A general tendency of this function, how it behaves as the coupling constant $\Gamma_{eff}$ increase, is obvious [6]: (1) The magnitude of $A_\alpha$ is much larger than that for equilibrium liquids, (2) $A_\alpha(t)$ is divided into two parts, both of which are increasing (in small times) and decreasing (in large times) functions of $t$, respectively, and the maximum appears around where these two functions are merged, and (3) the position and the value of this maximum significantly increases as $\Gamma_{eff}$ becomes larger. Compared with those for $N = 500$, the present results for $N = 4000$ are clearly seen much more smoothened in both the time dependent behaviour and the $\Gamma_{eff}$ dependence. In the shorter time scales, in which the function $A_\alpha$ is an increasing function of $t$, motions of atom are nearly of vibrations, not of diffusions. In other words, in this

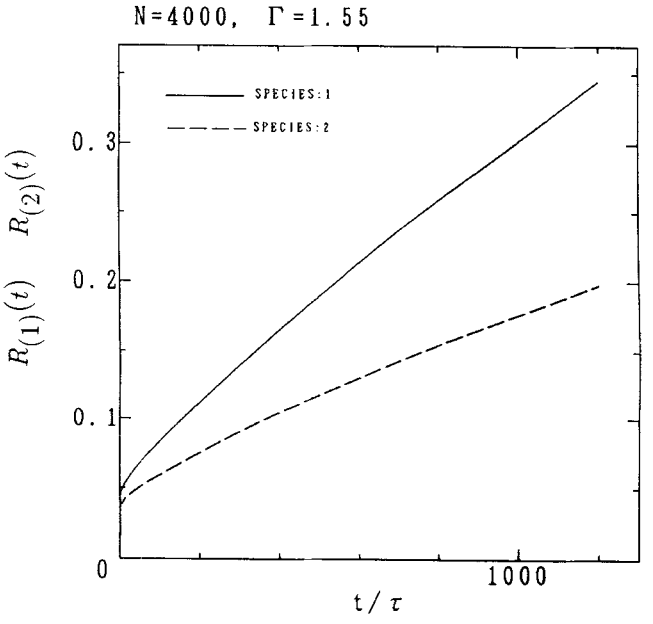


**Figure 10** The same as Figure 8, but for $\Gamma_{\text{eff}} = 1.55$.

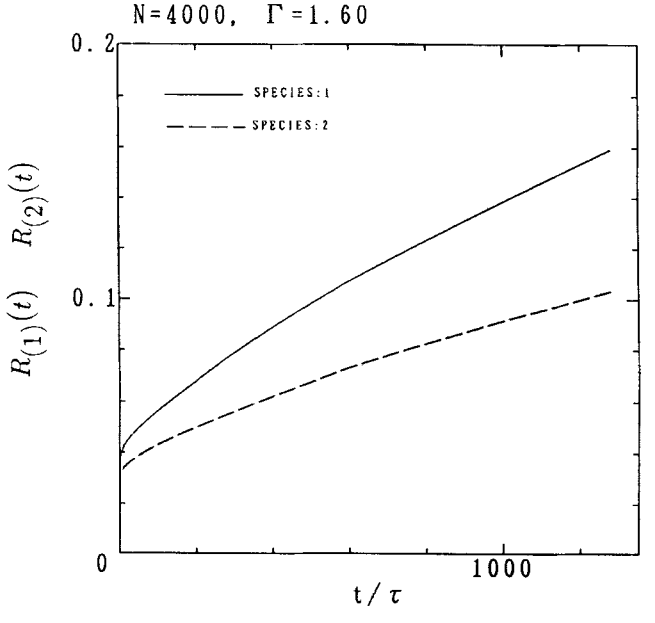


**Figure 11** The same as Figure 8, but for $\Gamma_{\text{eff}} = 1.60$.

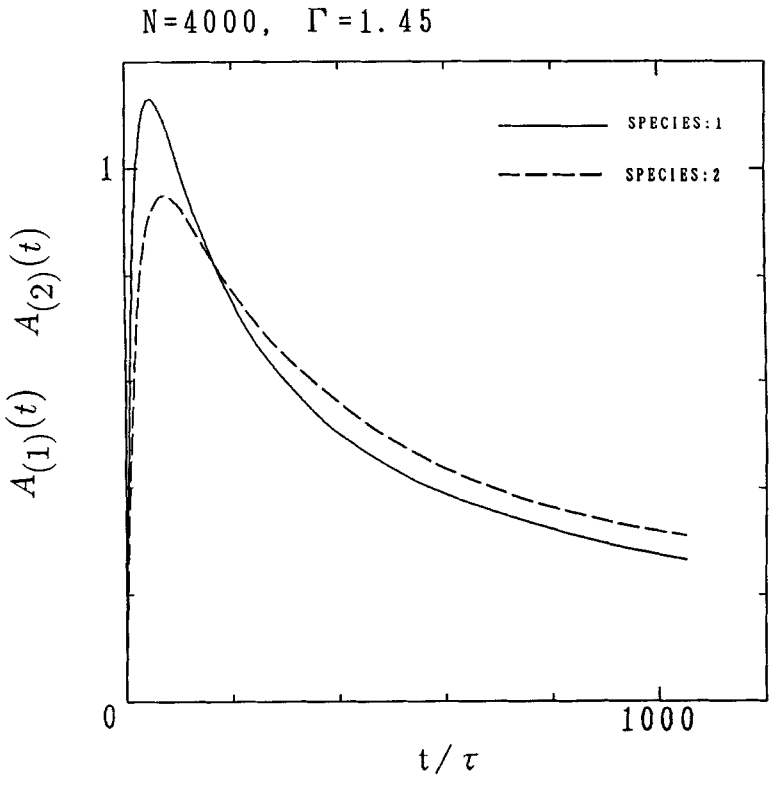


**Figure 12** Non-Gaussian parameters as a function of $t$ for $\Gamma_{eff} = 1.45$, for the lighter species (solid curve) and the heavier species (dashed curve), obtained from the MD simulations with $N = 4000$.

time scale is only $\beta$ dynamics essential. On the other hand, in the longer time scales, in which the function $A_\alpha(t)$ is a decreasing function of $t$, diffusions of atoms are possible. Therefore, in the latter $\alpha$ relaxation is dominant. From figures 12 to 15, it is interesting to note that in the short time scales $A_1$, that of lighter atoms, is always larger than $A_2$, that of heavier atoms, while in the long time scales, such relation becomes opposite, that is, $A_2$ is larger than $A_1$, though the physical origin for such result is not yet well understandable. It can be shown that the decay of $A_\alpha(t)$ for long times obeys a power law of $t$, i.e., $A(t) - A(\infty) \sim t^{-\delta}$, and thus the exponent $\delta$ can be calculated [5]. The value of $\delta$ is possibly related to $\beta$, since both deal with essentially the same slow dynamics.

## V CONCLUSIONS AND DISCUSSIONS

This paper discusses a long time or an intermediate time behaviour of the self-and full-parts density autocorrelation function in the time window of the order of $1000\tau$ ($\tau$ is the shortest microscopic time scale of the system), which is about one order of magnitude longer than our previous computations for the same function. The

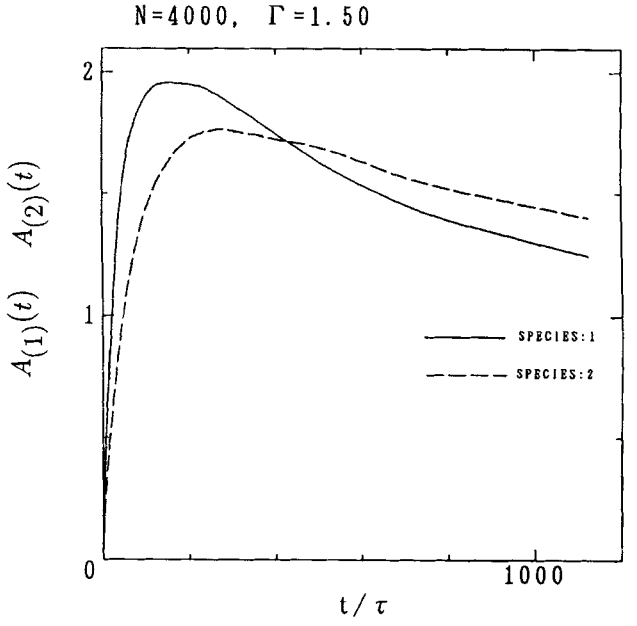


**Figure 13** The same as Figure 12, but for $\Gamma_{\text{eff}} = 1.50$.

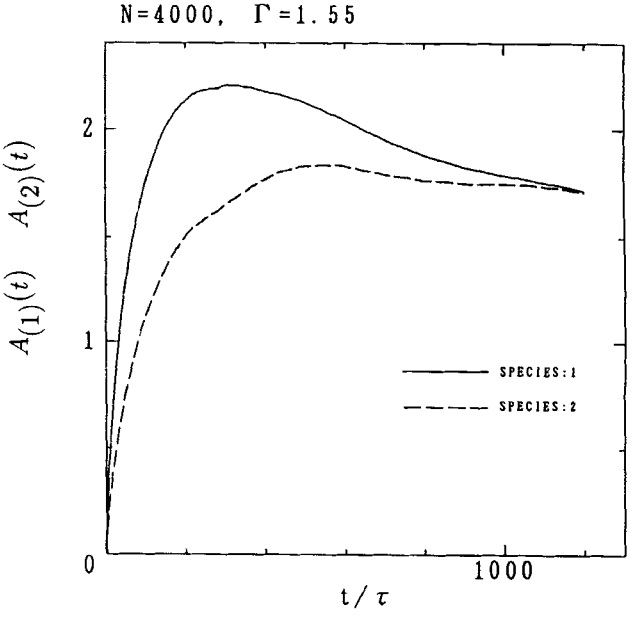


**Figure 14** The same as Figure 12, but for $\Gamma_{\text{eff}} = 1.55$.

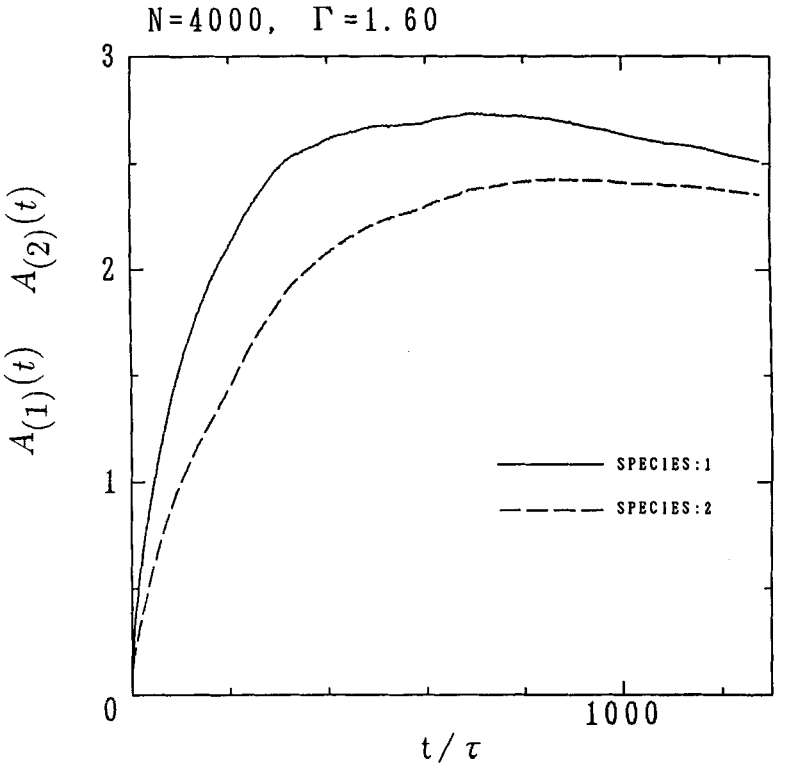


**Figure 15** The same as Figure 12, but for $\Gamma_{eff} = 1.60$.

present work also involves MD simulations for a larger system size than the previous ones. The results obtained by the present work are comparable with our previous results; for $\Gamma_{eff} > 1.45$ the density autocorrerlation $F_s(k, t)$ can perfectly be fitted by the stretched exponential function with $\beta < 1$ over the time steps of three figures except for a very short-time region. The present results on the values of $\beta$ with $N = 4000$ in the supercooled fluid phase for the binary soft-sphere model reveals a systematic dependence on the coupling constant $\Gamma_{eff}$, which is rather unclear from the calculations for $N = 500$. $\beta$ decreases significantly from unity as $\Gamma_{eff}$ increases, when it becomes larger than about 1.45.

Slow relaxations which we have discussed in the present work, as described in terms of the stretched exponential decay of the density fluctuations in the intermediate and long time windows, essentially correspond to the $\alpha$ relaxations in a supercooled fluid phase. Similar slow dynamics are also observed in the mean square displacements, as shown in Figures 8 through 11 and in the non Gaussian parameter, as shown in Figures 12 through 15. With the latter, the time window of our concern is separated into two, which are concerned with different dynamics, $\beta$ and $\alpha$ dynamics. Characterization and physical significances of these two dynamics are discussed more in detail with the trapping diffusion model in a separate paper of this volume.

*Acknowledgements*

The work was partly supported by a Grand-in-Aid from the ministry of Education, Science and Culture, Japan. Molecular dynamics computations were caried out with supercomputers at Kyoto University.

*References*

[1] For a recent review, see Y. Hiwatari, H. Miyagawa and T. Odagaki, "Dynamical singularities near the liquid-glass transition: Theory and molecular dynamics study", Solid State Ionics **47**, 179 (1991).
[2] H. Miyagawa and Y. Hiwatari, "Molecular-dynamics study of binary soft-sphere glasses: Quench-rate effects and aging effects", *Phys. Rev.*, **A40**, 6007 (1989).
[3] Y. Hiwatari and H. Miyagawa, "Molecular dynamics study of binary alloys near the glass transition" J. Non-cryst. *Solids*, **117/118**, 862 (1990).
[4] H. Miyagawa and Y. Hiwatari, "Molecular-dynamics study of the glass transition in a binary soft-sphere model", *Phys. Rev.*, **A44**, 8278 (1991).
[5] T. Odagaki and Y. Hiwatari, "Stochastic model for the glass transition of simple classical liquids", *Phys. Rev.*, **A41**, 929 (1990).
[6] T. Odagaki and Y. Hiwatari, "Gaussian-to-non-Gaussian transition in supercooled fluids", *Phys. Rev.*, **A43**, 1103 (1991).
[7] T. Odagaki and Y. Hiwatari, "Residence time distribution of a tracer atom in supercooled fluids", J. Phys.: Condens. *Matter*, **3**, 5191 (1991).
[8] T. Odagaki and Y. Hiwatari, "Apparent subdiffusive properties of a supercooled fluid", *Phys. Rev.*, **A46**, 1250 (1992).
[9] T. Odagaki and Y. Hiwatari, "Stochastic dynamics in a supercooled fluid", *AIP*, **256**, 115 (1992).
[10] Y. Hiwatari, H. Miyagawa, T. Muranaka and K. Uehara, "Molecular-dynamics study of highly supercooled liquids: Dynamical singularities near the liquid-glass transition", *AIP*, **256**, 155 (1992).
[11] B. Bernu, Y. Hiwatari and J.P. Hansen, "A molecular dynamics study of the glass transition in binary mixtures of soft spheres", *J. Phys. C*, **18**, L371 (1985).
[12] B. Bernu, J.P. Hansen, Y. Hiwatari and G. Pastore, "Soft-sphere model for the glass transition in binary alloys: Pair structure and self-diffusion", *Phys. Rev.*, **A36**, 4891 (1987).
[13] G. Pastore, B. Bernu, J.P. Hansen and Y. Hiwatari, "Soft-sphere model for the glass transition in binary alloys. II. Relaxation of the incoherent density-density correlation functions", *Phys. Rev.*, **A38**, 454 (1988).
[14] F. Mezei, W. Knaak and B. Farago, "Neutron spin-echo study of dynamic correlations near the liquid-glass transition", *Phys. Rev. Letters*, **58**, 571 (1987).
[15] F. Mezei, "Dynamic structure factor near the glass transition: Specific features", *AIP*, **256**, 53 (1992).
[16] A. Rahman, K.S. Singwi and A. Sjölander, "Theory of slow neutron scattering by liquids", *Phys. Rev.*, **126**, 986 (1962).